CHAPTER ONE

Introduction to the FDTD Method

As a major computational electromagnetics tool, the finite-difference time-domain (FDTD) method, proposed by K. S. Yee [1], is in widespread use as a solver for a variety of electromagnetic problems. Although the focus of this book is on simulation techniques and engineering applications, we begin by reviewing some of the basic concepts of the FDTD method, including update equations, numerical dispersion, stability properties, and the absorbing boundary condition. Readers desiring to gain additional details about the FDTD method are referred to the literature [2–9] on this subject.

1.1 THE FDTD METHOD

The FDTD method is a numerical technique based on the finite-difference concept used to solve Maxwell's equations for electric and magnetic field distributions in the time and spatial domains. The FDTD method utilizes the central difference approximation to discretize the two Maxwell's curl equations—Faraday's and Ampère's laws—in the time and spatial domains, and then solves the resulting equations numerically to derive the electric and magnetic field distributions at each time step using an explicit leapfrog scheme. The FDTD solution thus derived is second-order accurate and is stable if the time step satisfies the Courant condition.

In Yee's scheme [1], the computational domain is discretized by using a rectangular grid. The electric fields are located along the edges of the electric elements, while the magnetic fields are sampled at the centers of the electric element surfaces

Electromagnetic Simulation Techniques Based on the FDTD Method, By Wenhua Yu, Xiaoling Yang, Yongjun Liu, and Raj Mittra

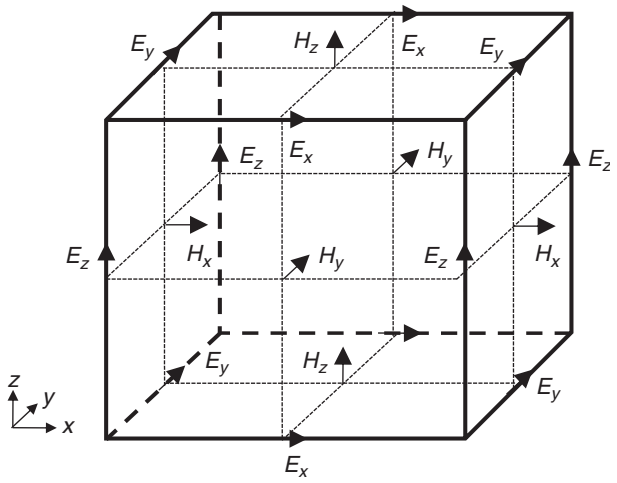

Figure 1.1 Position of the electric and magnetic fields in Yee's scheme.

and are oriented normal to these surfaces, this being consistent with the duality property of the electric and magnetic fields in Maxwell's equations. A typical electric unit is shown in Fig. 1.1.

The FDTD utilizes rectangular pulses as base functions in both the time and spatial domains, implying that the electric field is distributed uniformly along the edge of the electric element, while the distribution of the magnetic fields is uniform on the surface of the electric unit. In addition, in the time domain, the electric fields are sampled at times $n\ \Delta t$ and are assumed to be uniform in the time period $(n - \frac{1}{2}\ \Delta t)$ to $(n + \frac{1}{2}\ \Delta t)$. Similarly, the magnetic fields are sampled at $(n + \frac{1}{2}\ \Delta t)$ and are assumed to be uniform in the period $n\ \Delta t$ to $(n + 1)\ \Delta t$. The FDTD algorithm constructs a solution to the following two Maxwell curl equations:

$$\nabla \times \vec{E} = -\mu \frac{\partial \vec{H}}{\partial t} - \sigma_M \vec{H} \qquad \text{(Faraday's law)} \tag{1.1a}$$

$$\nabla \times \vec{H} = \varepsilon \frac{\partial \vec{E}}{\partial t} + \sigma \vec{E} \qquad \text{(Ampère's law)} \tag{1.1b}$$

In the Cartesian coordinate system, we can rewrite (1.1a) and (1.1b) as the following six coupled partial differential equations:

$$\frac{\partial H_x}{\partial t} = \frac{1}{\mu_x}\left(\frac{\partial E_y}{\partial z} - \frac{\partial E_z}{\partial y} - \sigma_{Mx} H_x\right) \tag{1.2a}$$

$$\frac{\partial H_y}{\partial t} = \frac{1}{\mu_y}\left(\frac{\partial E_z}{\partial x} - \frac{\partial E_x}{\partial z} - \sigma_{My} H_y\right) \tag{1.2b}$$

$$\frac{\partial H_z}{\partial t} = \frac{1}{\mu_z}\left(\frac{\partial E_x}{\partial y} - \frac{\partial E_y}{\partial x} - \sigma_{Mz} H_z\right) \tag{1.2c}$$

$$\frac{\partial E_x}{\partial t} = \frac{1}{\varepsilon_x}\left(\frac{\partial H_z}{\partial y} - \frac{\partial H_y}{\partial z} - \sigma_x E_x\right) \tag{1.2d}$$

$$\frac{\partial E_y}{\partial t} = \frac{1}{\varepsilon_y}\left(\frac{\partial H_x}{\partial z} - \frac{\partial H_z}{\partial x} - \sigma_y E_y\right) \tag{1.2e}$$

$$\frac{\partial E_z}{\partial t} = \frac{1}{\varepsilon_z}\left(\frac{\partial H_y}{\partial x} - \frac{\partial H_x}{\partial y} - \sigma_z E_z\right) \tag{1.2f}$$

where ε and σ, μ and σ_M are the electric and magnetic parameters of the material, respectively. The anisotropic material can be described by using different values of dielectric parameters along the different directions. Equations (1.2a) to (1.2f) form the foundation of the FDTD algorithm for modeling the interaction of electromagnetic waves with arbitrary three-dimensional objects embedded in arbitrary media and excited by a given excitation source. Using the conventional notations, discretized fields in the time and spatial domains can be written in the following format:

$$E_x^n(i+\tfrac{1}{2}, j, k) = E_x((i+\tfrac{1}{2})\ \Delta x, j\ \Delta y, k\ \Delta z, n\ \Delta t) \tag{1.3a}$$

$$E_y^n(i, j+\tfrac{1}{2}, k) = E_y(i\ \Delta x, (j+\tfrac{1}{2})\ \Delta y, k\ \Delta z, n\ \Delta t) \tag{1.3b}$$

$$E_z^n(i, j, k+\tfrac{1}{2}) = E_z(i\ \Delta x, j\ \Delta y, (k+\tfrac{1}{2})\ \Delta z, n\ \Delta t) \tag{1.3c}$$

$$\begin{aligned} &H_x^{n+\frac{1}{2}}(i, j+\tfrac{1}{2}, k+\tfrac{1}{2}) \\ &\quad = H_x(i\ \Delta x, (j+\tfrac{1}{2})\ \Delta y, (k+\tfrac{1}{2})\ \Delta z, (n+\tfrac{1}{2})\ \Delta t) \end{aligned} \tag{1.3d}$$

$$\begin{aligned} &H_y^{n+\frac{1}{2}}(i+\tfrac{1}{2}, j, k+\tfrac{1}{2}) \\ &\quad = H_y((i+\tfrac{1}{2})\ \Delta x, j\ \Delta y, (k+\tfrac{1}{2})\ \Delta z, (n+\tfrac{1}{2})\ \Delta t) \end{aligned} \tag{1.3e}$$

$$\begin{aligned} &H_z^{n+\frac{1}{2}}(i+\tfrac{1}{2}, j+\tfrac{1}{2}, k) \\ &\quad = H_z((i+\tfrac{1}{2})\ \Delta x, (j+\tfrac{1}{2})\ \Delta y, k\ \Delta z, (n+\tfrac{1}{2})\ \Delta t) \end{aligned} \tag{1.3f}$$

It is useful to note that the electric and magnetic fields in the discretized version are staggered in both time and space. For example, the electric and magnetic fields are sampled at the time steps $n\ \Delta t$ and $(n+\frac{1}{2})\ \Delta t$, respectively, and are also displaced from each other in space, as shown in Fig. 1.1. Therefore, we need to interpolate the sampled electric and magnetic fields in order to measure the electric and magnetic fields in the continuous spatial and time domains. Ignoring this field-sampling offset in the Fourier transforms may result in a significant error at high frequencies.

Using the notations in (1.3a) to (1.3f), we can represent Maxwell's equations (1.2a) to (1.2f) in the following explicit formats [2]:

$$H_x^{n+1/2}(i, j+\tfrac{1}{2}, k+\tfrac{1}{2}) = \frac{\mu_x - 0.5\Delta t\sigma_{Mx}}{\mu_x + 0.5\Delta t\sigma_{Mx}} H_x^{n-1/2}(i, j+\tfrac{1}{2}, k+\tfrac{1}{2}) + \frac{\Delta t}{\mu_x + 0.5\Delta t\sigma_{Mx}} \left[\frac{E_y^n(i, j+\tfrac{1}{2}, k+1) - E_y^n(i, j+\tfrac{1}{2}, k)}{\Delta z} - \frac{E_z^n(i, j+1, k+\tfrac{1}{2}) - E_z^n(i, j, k+\tfrac{1}{2})}{\Delta y} \right] \tag{1.4a}$$

$$H_y^{n+1/2}(i+\tfrac{1}{2}, j, k+\tfrac{1}{2}) = \frac{\mu_y - 0.5\Delta t\sigma_{My}}{\mu_y + 0.5\Delta t\sigma_{My}} H_y^{n-1/2}(i+\tfrac{1}{2}, j, k+\tfrac{1}{2}) + \frac{\Delta t}{\mu_y + 0.5\Delta t\sigma_{My}} \left[\frac{E_z^n(i+1, j, k+\tfrac{1}{2}) - E_z^n(i, j, k+\tfrac{1}{2})}{\Delta x} - \frac{E_x^n(i+\tfrac{1}{2}, j, k+1) - E_x^n(i+\tfrac{1}{2}, j, k)}{\Delta z} \right] \tag{1.4b}$$

$$H_z^{n+1/2}(i+\tfrac{1}{2}, j+\tfrac{1}{2}, k) = \frac{\mu_z - 0.5\Delta t\sigma_{Mz}}{\mu_z + 0.5\Delta t\sigma_{Mz}} H_z^{n-1/2}(i+\tfrac{1}{2}, j+\tfrac{1}{2}, k) + \frac{\Delta t}{\mu_z + 0.5\Delta t\sigma_{Mz}} \left[\frac{E_x^n(i+\tfrac{1}{2}, j+1, k) - E_x^n(i+\tfrac{1}{2}, j, k)}{\Delta y} - \frac{E_y^n(i+1, j+\tfrac{1}{2}, k) - E_y^n(i, j+\tfrac{1}{2}, k)}{\Delta x} \right] \tag{1.4c}$$

$$E_x^{n+1}(i+\tfrac{1}{2}, j, k) = \frac{\varepsilon_x - 0.5\Delta t\sigma_x}{\varepsilon_x + 0.5\Delta t\sigma_x} E_x^n(i+\tfrac{1}{2}, j, k) + \frac{\Delta t}{\varepsilon_x + 0.5\Delta t\sigma_x} \left[\frac{H_z^{n+1/2}(i+\tfrac{1}{2}, j+\tfrac{1}{2}, k) - H_z^{n+1/2}(i+\tfrac{1}{2}, j-\tfrac{1}{2}, k)}{\Delta y} - \frac{H_y^{n+1/2}(i+\tfrac{1}{2}, j, k+\tfrac{1}{2}) - H_y^{n+1/2}(i+\tfrac{1}{2}, j, k-\tfrac{1}{2})}{\Delta z} \right] \tag{1.4d}$$

$$E_y^{n+1}(i, j+\tfrac{1}{2}, k) = \frac{\varepsilon_y - 0.5\Delta t\sigma_y}{\varepsilon_y + 0.5\Delta t\sigma_y} E_y^n(i, j+\tfrac{1}{2}, k)$$
$$+ \frac{\Delta t}{\varepsilon_y + 0.5\Delta t\sigma_y}\left[\frac{H_x^{n+1/2}(i, j+\frac{1}{2}, k+\frac{1}{2}) - H_x^{n+1/2}(i, j+\frac{1}{2}, k-\frac{1}{2})}{\Delta z}\right.$$
$$\left. - \frac{H_z^{n+1/2}(i+\frac{1}{2}, j+\frac{1}{2}, k) - H_z^{n+1/2}(i-\frac{1}{2}, j+\frac{1}{2}, k)}{\Delta x}\right] \tag{1.4e}$$

$$E_z^{n+1}(i, j, k+\tfrac{1}{2}) = \frac{\varepsilon_z - 0.5\Delta t\sigma_z}{\varepsilon_z + 0.5\Delta t\sigma_z} E_z^n(i, j, k+\tfrac{1}{2})$$
$$+ \frac{\Delta t}{\varepsilon_z + 0.5\Delta t\sigma_z}\left[\frac{H_y^{n+1/2}(i+\frac{1}{2}, j, k+\frac{1}{2}) - H_y^{n+1/2}(i-\frac{1}{2}, j, k+\frac{1}{2})}{\Delta x}\right.$$
$$\left. - \frac{H_x^{n+1/2}(i, j+\frac{1}{2}, k+\frac{1}{2}) - H_x^{n+1/2}(i, j-\frac{1}{2}, k+\frac{1}{2})}{\Delta y}\right] \tag{1.4f}$$

We point out that for simplicity we have omitted the explicit indices for the material parameters, which share the same indices with the corresponding field components. Equations (1.4a) through (1.4f) do not contain any explicit boundary information, and we need to augment them with an appropriate boundary condition in order to truncate the computational domain. In the FDTD simulation, some of the commonly used boundary conditions include those associated with the perfect electric conductor (PEC), the perfect magnetic conductor (PMC), the absorbing boundary condition (ABC), and the periodic boundary condition (PBC). In addition to the boundary conditions above, we also need to handle the interfaces between different media in an inhomogeneous environment. In accordance with the assumption of the locations of the electric and magnetic fields, the magnetic field is located along the line segment joining the two centers of adjacent cells. Consequently, the effective magnetic parameter corresponding to this magnetic field is the weighted average of the parameters of the material that fills the two adjacent cells. Unlike the magnetic field, the loop used to compute the electric field is likely to be distributed among four adjacent cells; therefore, the effective electric parameter corresponding to this electric field is equal to the weighted average of electric parameters of the material that fills these four cells. In addition, the curved PEC and dielectric surfaces require use of the conformal FDTD technique [3,4,9,10] for accurate modeling.

In recent years, research on the FDTD method has focused on the following three topics: improving the conventional FDTD algorithm and employing the conformal

version instead to reduce the error introduced by the staircasing approximation; using a subgridding scheme in the FDTD technique to increase the local resolution [11–13], and employing the alternative direction implicit (ADI) FDTD algorithm [14,15] to increase the time step. In addition, new FDTD algorithms such as the multiresolution time-domain (MRTD) method [16] and the pseudospectrum time-domain (PSTD) technique [17] have been proposed with a view to lowering the spatial sampling. Yet another strategy, which has been found to be more robust than the MRTD and PSTD techniques, is to parallelize the conformal code [18,19] and enhance it either with subgridding, the ADI algorithm, or both. The parallel FDTD algorithm gains computational efficiency by distributing the burden on a cluster. It also enables one to solve large problems that could be beyond the scope of a single processor because of central processing unit time limitations.

1.2 NUMERICAL DISPERSION

If a medium is dispersive, the propagation velocities of electromagnetic waves will vary with frequency in such a medium. In a nondispersive medium—for example, in free space—the radian frequency and the wave numbers satisfy the relationship

$$\left(\frac{\omega}{c}\right)^2 = k_x^2 + k_y^2 + k_z^2 \tag{1.5}$$

where k_x, k_y, and k_z are the propagation constants along the x-, y-, and z-directions, respectively. Even when the medium is nondispersive, electromagnetic waves inside the FDTD mesh travel along different directions at different speeds, a phenomenon known as the *numerical dispersion error*. This error is a function of the FDTD cell size and shape as well as the shape of the differencing format used to discretize the differential equations.

We now proceed to investigate the numerical dispersion characteristics of the FDTD method in the Cartesian coordinate system. We begin by representing a plane wave function as

$$\psi(x, y, z, t) = \psi_0 \exp[j(\omega t - k_x x - k_y y - k_z z)] \tag{1.6}$$

where the radian frequency $\omega = 2\pi f$. If the discretizations in the x-, y-, and z-directions and the time step are Δx, Δy, Δz, and Δt, respectively, the expression in (1.6) can be written as

$$\psi^n(I, J, K) = \psi_0 \exp[j(\omega n\ \Delta t - k_x I\ \Delta x - k_y J\ \Delta y - k_z K\ \Delta z)] \tag{1.7}$$

where n, I, J, and K are the indices in time and space, respectively. In free space, electromagnetic waves satisfy the following wave equation:

$$\left(\frac{\partial^2}{\partial x^2} + \frac{\partial^2}{\partial y^2} + \frac{\partial^2}{\partial z^2} - \frac{1}{c^2}\frac{\partial^2}{\partial t^2}\right)\psi = 0 \tag{1.8}$$

where c is the velocity of light in free space. Using central differencing in both the time and spatial domains, we can discretize (1.8) to get

$$\begin{aligned}
&\frac{\psi^n(i+1,j,k)-2\psi^n(i,j,k)+\psi^n(i-1,j,k)}{\Delta x^2}\\
&\quad+\frac{\psi^n(i,j+1,k)-2\psi^n(i,j,k)+\psi^n(i,j-1,k)}{\Delta y^2}\\
&\quad+\frac{\psi^n(i,j,k+1)-2\psi^n(i,j,k)+\psi^n(i,j,k-1)}{\Delta z^2}\\
&\quad=\frac{\psi^{n+1}(i,j,k)-2\psi^n(i,j,k)+\psi^{n-1}(i,j,k)}{\Delta t^2}
\end{aligned} \tag{1.9}$$

Substituting (1.7) into (1.9), we have

$$\begin{aligned}
&\left(\frac{1}{c\ \Delta t}\sin\frac{\omega\ \Delta t}{2}\right)^2\\
&\quad=\left(\frac{1}{\Delta x}\sin\frac{k_x\ \Delta x}{2}\right)^2+\left(\frac{1}{\Delta y}\sin\frac{k_y\ \Delta y}{2}\right)^2+\left(\frac{1}{\Delta z}\sin\frac{k_z\ \Delta z}{2}\right)^2
\end{aligned} \tag{1.10}$$

It is evident that (1.10) reduces to (1.5) as $\Delta x \to 0$, $\Delta y \to 0$, and $\Delta z \to 0$, implying that the numerical dispersion error decreases when the cell size is reduced. In addition, the numerical dispersion error is different along different propagation directions, and we illustrate this phenomenon next through a simple two-dimensional example of propagation in a uniform mesh (i.e., for $\Delta x = \Delta y$). We assume that a line source oriented along the z-direction is located in free space. In Fig. 1.2 we plot the distribution of its radiated field E_z in the $x-y$ plane. It is evident that the numerical dispersion error is smaller along the diagonals when $\phi = 45^\circ, 135^\circ, 225^\circ$, and 315° than in other directions.

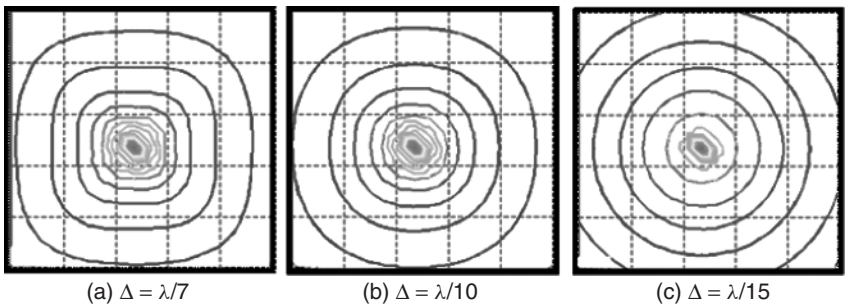

Figure 1.2 Numerical dispersion of the FDTD method.

1.3 STABILITY ANALYSIS

One of the critical issues that we must address when developing a code that utilizes the marching-on-time technique is the stability of the algorithm. The stability characteristic of the FDTD algorithm depends on the nature of the physical model, the differencing technique employed, and the quality of the mesh structure. To understand the nature of the stability characteristic, we solve (1.10) for ω to get

$$\omega = \frac{2}{\Delta t}\sin^{-1}\left(c\ \Delta t\sqrt{\frac{1}{\Delta x^2}\sin^2\frac{k_x\ \Delta x}{2}+\frac{1}{\Delta y^2}\sin^2\frac{k_y\ \Delta y}{2}+\frac{1}{\Delta z^2}\sin^2\frac{k_z\ \Delta z}{2}}\right) \tag{1.11}$$

If ω is an imaginary number, we know from (1.6) that the electromagnetic waves will either attenuate rapidly to zero or grow exponentially and become divergent, depending on whether the imaginary part is positive or negative. To ensure that ω is a real number instead, the expression inside parentheses in (1.11) must satisfy the condition

$$c\ \Delta t\sqrt{\frac{1}{\Delta x^2}\sin^2\frac{k_x\ \Delta x}{2}+\frac{1}{\Delta y^2}\sin^2\frac{k_y\ \Delta y}{2}+\frac{1}{\Delta z^2}\sin^2\frac{k_z\ \Delta z}{2}} \le 1 \tag{1.12}$$

Since the maximum possible value of the sine-squared term under the square root is 1, the time step must satisfy

$$\Delta t \le \frac{1}{c\sqrt{1/\Delta x^2+1/\Delta y^2+1/\Delta z^2}} \tag{1.13}$$

for the solution to be stable. The criterion above is called the *stability condition for the FDTD method* and is referred to as the *Courant condition* (or the *Courant, Friedrichs, and Lewy criterion*) [19]. Equation (1.13) indicates that the time step is determined by the cell sizes in the x-, y-, and z-directions and the speed of light in the medium.

To help the reader gain further physical insight into (1.13), we simplify (1.13) to a one-dimensional case, where the Courant condition is simplified to $c\ \Delta t \le \Delta x$. The time required for the field to propagate from the nth to the $(n+1)$th node is obviously $\Delta t = \Delta x/c$. In FDTD simulations, let us suppose that we choose a time step $\Delta t > \Delta x/c$. Then the algorithm yields a nonzero field value before the wave can reach the $(n+1)$th node, traveling at the speed of light. This would violate causality and result in an unstable solution.

1.4 BOUNDARY CONDITIONS

It is well known that boundary conditions play a very important role in FDTD simulations, because they are used to truncate the computational domain when modeling an open region problem. Although the original FDTD algorithm was proposed as early as 1966, it was not really used to solve practical problems until the early 1980s, when Mur's absorbing boundary [20] was proposed. Although Mur's absorbing boundary condition is relatively simple, and it has been used successfully to solve many engineering problems, it has room for improvement in terms of the accuracy of the solution it generates. To improve its accuracy, Mei and Fang [21] introduced the *superabsorption technique*, and Chew [25] proposed employing Liao's boundary condition, both of which exhibit better characteristics than those of Mur, especially for obliquely incident waves. However, many of these absorbing boundary conditions were found to suffer from either an instability problem or an inaccurate solution, and the quest for robust and effective boundary conditions continued unabated until the perfectly matched layer (PML) was introduced by Berenger [23], and several other versions [24–27] have been proposed since then. In contrast to the other boundary conditions, such as those of Mur and Liao, an infinite PML can absorb the incoming waves at all frequencies as well as for all incident angles. The perfect electric conductor (PEC) is a natural boundary for electromagnetic waves, since it totally reflects the waves falling on it. When the PEC condition is applied to truncate the FDTD computational domain, it simply forces the tangential electric fields on the domain boundary to be zero. In common with the PEC, the perfect magnetic conductor (PMC) is also a natural type of boundary condition for electromagnetic waves, and it is also totally reflecting. However, unlike the PEC, the PMC is not physical but is merely an artifice. Both the PEC and PMC are often used to take advantage of the symmetry of the object geometry with a view to reducing the size of the computational domain. In this section we focus on the time convolution PML [27], one of the most popular PML formats. Although the PML is named to be an absorbing boundary condition, in fact, it is an anisotropic material (albeit mathematical) which is inserted in the periphery of the computational domain to absorb the outgoing waves.

Before introducing the PML boundary conditions, we investigate their role in FDTD simulations. In the FDTD method, Maxwell's equations that govern the relationship between the electric and magnetic fields in the time and spatial domains are translated into difference equations, which do not explicitly contain any boundary information. It is necessary, therefore, to combine the difference equations with the appropriate boundary conditions in order to carry out the mesh truncation as a preamble to solving these equations. Generally speaking, we require two types of boundary conditions in FDTD simulations: the interface condition between different media, and the outer boundary condition for mesh truncation. In this chapter we discuss only the latter: the boundary that is used to truncate the computational domain.

The time-convolution PML is based on the stretched coordinate PML [25,26], and the six coupled Maxwell's equations in the time-convolution PML can be written in the following form:

$$j\omega\varepsilon\tilde{E}_x + \sigma_x\tilde{E}_x = \frac{1}{S_y}\frac{\partial\tilde{H}_z}{\partial y} - \frac{1}{S_z}\frac{\partial\tilde{H}_y}{\partial z} \tag{1.14a}$$

$$j\omega\varepsilon\tilde{E}_y + \sigma_y\tilde{E}_y = \frac{1}{S_z}\frac{\partial\tilde{H}_x}{\partial z} - \frac{1}{S_x}\frac{\partial\tilde{H}_z}{\partial x} \tag{1.14b}$$

$$j\omega\varepsilon\tilde{E}_z + \sigma_z\tilde{E}_z = \frac{1}{S_x}\frac{\partial\tilde{H}_y}{\partial x} - \frac{1}{S_y}\frac{\partial\tilde{H}_x}{\partial y} \tag{1.14c}$$

$$j\omega\mu_x\tilde{H}_x + \sigma_{Mx}\tilde{H}_x = \frac{1}{S_z}\frac{\partial\tilde{E}_y}{\partial z} - \frac{1}{S_y}\frac{\partial\tilde{E}_z}{\partial y} \tag{1.14d}$$

$$j\omega\mu_y\tilde{H}_y + \sigma_{My}\tilde{H}_y = \frac{1}{S_x}\frac{\partial\tilde{E}_z}{\partial x} - \frac{1}{S_z}\frac{\partial\tilde{E}_x}{\partial z} \tag{1.14e}$$

$$j\omega\mu_z\tilde{H}_z + \sigma_{Mz}\tilde{H}_z = \frac{1}{S_y}\frac{\partial\tilde{E}_x}{\partial y} - \frac{1}{S_x}\frac{\partial\tilde{E}_y}{\partial x} \tag{1.14f}$$

To derive the update equations for the time-convolution PML from (1.14a), we first take its Laplace transform to obtain the following equation in the time domain:

$$\varepsilon_x\frac{\partial E_x}{\partial t} + \sigma_x E_x = \bar{S}_y(t) * \frac{\partial H_z}{\partial y} - \bar{S}_z(t) * \frac{\partial H_y}{\partial z} \tag{1.15}$$

where $\bar{S}_y$ and $\bar{S}_z$ are the Laplace transforms of $1/S_y$ and $1/S_z$, respectively.

The time-convolution PML is derived by converting (1.15) to a form that is suitable for explicit updating. Furthermore, to overcome the shortcomings of the split-field and unsplit PMLs insofar as the effectiveness at low frequencies and the absorption of the surface waves are concerned, we modify S_x, S_y, and S_z as follows:

$$S_x = K_x + \frac{\sigma_{x,\mathrm{PML}}}{\alpha_x + j\omega\varepsilon_0}, \qquad S_y = K_y + \frac{\sigma_{y,\mathrm{PML}}}{\alpha_y + j\omega\varepsilon_0}, \qquad S_z = K_z + \frac{\sigma_{\mathrm{z,PML}}}{\alpha_z + j\omega\varepsilon_0}$$

where $\alpha_{x,y,z}$ and $\sigma_{x,y,z,\mathrm{PML}}$ are real numbers and K is greater than 1. $\bar{S}_x$, $\bar{S}_y$, and $\bar{S}_z$ can be obtained from the Laplace transforms:

$$\bar{S}_x = \frac{\delta(t)}{K_x} - \frac{\sigma_x}{\varepsilon_0 K_x}\exp\left[-\left(\frac{\sigma_{x,\mathrm{PML}}}{\varepsilon_0 K_x} + \frac{\alpha_{x,\mathrm{PML}}}{\varepsilon_0}\right)tu(t)\right] = \frac{\delta(t)}{K_x} + \xi_x(t) \tag{1.16}$$

$$\bar{S}_y = \frac{\delta(t)}{K_y} - \frac{\sigma_y}{\varepsilon_0 K_y}\exp\left[-\left(\frac{\sigma_{y,\mathrm{PML}}}{\varepsilon_0 K_y} + \frac{\alpha_{y,\mathrm{PML}}}{\varepsilon_0}\right)tu(t)\right] = \frac{\delta(t)}{K_y} + \xi_y(t) \tag{1.17}$$

$$\bar{S}_z = \frac{\delta(t)}{K_z} - \frac{\sigma_z}{\varepsilon_0 K_z} \exp\left[-\left(\frac{\sigma_{z,\mathrm{PML}}}{\varepsilon_0 K_z} + \frac{\alpha_{z,\mathrm{PML}}}{\varepsilon_0} \right) t u(t) \right] = \frac{\delta(t)}{K_z} + \xi_z(t) \tag{1.18}$$

where $\delta(t)$ and $u(t)$ are an impulse function and a step function, respectively. Substituting (1.17) and (1.18) into (1.15), we have

$$\varepsilon_x \varepsilon_0 \frac{\partial E_x}{\partial t} + \sigma_x E_x = \frac{1}{K_y} \frac{\partial H_z}{\partial y} - \frac{1}{K_z} \frac{\partial H_y}{\partial z} + \xi_y(t) * \frac{\partial H_z}{\partial y} - \xi_z(t) * \frac{\partial H_y}{\partial z} \tag{1.19}$$

It is not numerically efficient to compute the convolution appearing directly in (1.19), and to address this issue and calculate it efficiently, we introduce a quantity $Z_{0y}(m)$:

$$\begin{aligned} Z_{0y}(m) &= \int_{m\Delta t}^{(m+1)\Delta t} \xi_y(\tau)\, d\tau \\ &= -\frac{\sigma_y}{\varepsilon_0 K_y^2} \int_{m\Delta t}^{(m+1)\Delta t} \exp\left[-\left(\frac{\sigma_{y,\mathrm{PML}}}{\varepsilon_0 K_y} + \frac{\alpha_{y,\mathrm{PML}}}{\varepsilon_0} \right) \tau \right] d\tau \\ &= a_y \exp\left[-\left(\frac{\sigma_{y,\mathrm{PML}}}{K_y} + \alpha_{y,\mathrm{PML}} \right) \frac{m\ \Delta t}{\varepsilon_0} \right] \end{aligned} \tag{1.20}$$

where

$$a_y = \frac{\sigma_{y,\mathrm{PML}}}{\sigma_{y,\mathrm{PML}} K_y + K_y^2 \alpha_y} \left(\exp\left[-\left(\frac{\sigma_{y,\mathrm{PML}}}{K_y} + \alpha_y \right) \frac{m\ \Delta t}{\varepsilon_0} \right] - 1 \right) \tag{1.21}$$

A similar expression can be derived for $Z_{0z}(m)$. Using (1.20) and (1.21), (1.19) can be written as

$$\begin{aligned} &\varepsilon_x \varepsilon_0 \frac{E_x^{n+1}(i+\frac{1}{2}, j, k) - E_x^n(i+\frac{1}{2}, j, k)}{\Delta t} + \sigma_x \frac{E_x^{n+1}(i+\frac{1}{2}, j, k) + E_x^n(i+\frac{1}{2}, j, k)}{2} \\ &= \frac{H_z^{n+1/2}(i+\frac{1}{2}, j+\frac{1}{2}, k) - H_z^{n+1/2}(i+\frac{1}{2}, j-\frac{1}{2}, k)}{K_y\ \Delta y} \\ &\quad - \frac{H_y^{n+1/2}(i+\frac{1}{2}, j, k+\frac{1}{2}) - H_y^{n+1/2}(i+\frac{1}{2}, j, k-\frac{1}{2})}{K_z\ \Delta z} \\ &\quad + \sum_{m=0}^{N-1} Z_{0y}(m) \frac{H_z^{n-m+1/2}(i+\frac{1}{2}, j+\frac{1}{2}, k) - H_z^{n-m+1/2}(i+\frac{1}{2}, j-\frac{1}{2}, k)}{K_y\ \Delta y} \\ &\quad - \sum_{m=0}^{N-1} Z_{0z}(m) \frac{H_y^{n-m+1/2}(i+\frac{1}{2}, j, k+\frac{1}{2}) - H_y^{n-m+1/2}(i+\frac{1}{2}, j, k-\frac{1}{2})}{K_z\ \Delta z} \end{aligned} \tag{1.22}$$

Finally, the update formula of (1.22) takes the form

$$\varepsilon_x\varepsilon_0\frac{E_x^{n+1}(i+\frac{1}{2},j,k)-E_x^{n}(i+\frac{1}{2},j,k)}{\Delta t}+\sigma_x\frac{E_x^{n+1}(i+\frac{1}{2},j,k)+E_x^{n}(i+\frac{1}{2},j,k)}{2}$$
$$=\frac{H_z^{n+1/2}(i+\frac{1}{2},j+\frac{1}{2},k)-H_z^{n+1/2}(i+\frac{1}{2},j-\frac{1}{2},k)}{K_y\ \Delta y}$$
$$-\frac{H_y^{n+1/2}(i+\frac{1}{2},j,k+\frac{1}{2})-H_y^{n+1/2}(i+\frac{1}{2},j,k-\frac{1}{2})}{K_z\ \Delta z}$$
$$+\psi_{\text{exy}}^{n+1/2}(i+\frac{1}{2},j,k)-\psi_{\text{exz}}^{n+1/2}(i+\frac{1}{2},j,k) \tag{1.23}$$

where

$$\psi_{\text{exy}}^{n+1/2}(i+\tfrac{1}{2},j,k)=b_y\psi_{\text{exy}}^{n-1/2}(i+\tfrac{1}{2},j,k)+a_y\frac{H_z^{n+1/2}(i+\frac{1}{2},j+\frac{1}{2},k)-H_z^{n+1/2}(i+\frac{1}{2},j-\frac{1}{2},k)}{\Delta y} \tag{1.24}$$

$$\psi_{\text{exz}}^{n+1/2}(i+\tfrac{1}{2},j,k)=b_z\psi_{\text{exz}}^{n-1/2}(i+\tfrac{1}{2},j,k)+a_z\frac{H_y^{n+1/2}(i+\frac{1}{2},j,k+\frac{1}{2})-H_y^{n+1/2}(i+\frac{1}{2},j,k-\frac{1}{2})}{\Delta z} \tag{1.25}$$

$$b_x=\exp\left[-\left(\frac{\sigma_{x,\text{PML}}}{K_x}+\alpha_x\right)\left(\frac{\Delta t}{\varepsilon_0}\right)\right] \tag{1.26a}$$

$$b_y=\exp\left[-\left(\frac{\sigma_{y,\text{PML}}}{K_y}+\alpha_y\right)\left(\frac{\Delta t}{\varepsilon_0}\right)\right] \tag{1.26b}$$

$$b_z=\exp\left[-\left(\frac{\sigma_{z,\text{PML}}}{K_z}+\alpha_z\right)\left(\frac{\Delta t}{\varepsilon_0}\right)\right] \tag{1.26c}$$

Equation (1.23) is the desirable update equation that we have been seeking to retain the advantages of the unsplit PML, and at the same time, overcome its drawback. In common with the conventional FDTD method, electric field updating inside the PML region requires only the magnetic fields around it and the value of ψ at the previous time step. The same statement is also true for the magnetic field update. The time-domain convolution PML does not require additional information exchange in the parallel FDTD simulation over and above that in the conventional FDTD method.

Suppose that x is the distance measured from the outer boundary of the computational domain; then the conductivity distribution in the PML region is given by

$$\sigma(x) = \sigma_{\max}\left(\frac{d-x}{d}\right)^m \tag{1.27}$$

where the index m is taken to be either 2 or 4. In addition, in (1.27), d is the thickness of the PML region and $\sigma_{\max}$ is the maximum value of the conductivity, which can be expressed as

$$\sigma_{\max} = \frac{m+1}{200\pi\sqrt{\varepsilon_r}\ \Delta x} \tag{1.28}$$

Suppose that y is a distance measured from the outer boundary of the computational domain; the distribution of K_y is given by

$$K_y(y) = 1 + (K_{\max} - 1)\frac{|d-y|^m}{d^m} \tag{1.29}$$

Implementation of the time-convolution PML in the FDTD code is relatively simpler than for most other types of PMLs. Also, this type of PML does not depend on the properties of the materials being simulated. In addition, it shows performance at low frequencies.

Numerical experiments have proven that the performance of the PML is not very sensitive to the choice of K. For example, we do not observe any significant variation in the reflection property of the PML when the value of $K_{\max}$ varies from 1 to 15. However, the value of α in (1.21) and (1.26) plays an important role in determining the reflection level of the time-domain convolution PML. We have found, by carrying out numerical experiments, that the value of α to be chosen depends not only on the cell size inside the PML region but also on the width of the excitation pulse used in the FDTD simulation; furthermore, it is not possible to employ a single α value to cover all possible cell sizes and pulse shapes that we might use. Fortunately, however, we can easily find a suitable value of α for a narrow range of cell size and pulse shape. For example, for a Gaussian pulse modulated with a sinusoidal function ($f_{3\text{dB}} = 1$ GHz and $f_{\text{modulation}} = 1$ GHz), the highest frequency of spectrum of the excitation pulse is about 5 GHz, and the cell sizes in the FDTD simulations are selected to be 0.0001 to 0.006 m. For this case, the value of α can be chosen as follows:

$$\alpha_x = \eta\frac{0.06}{300\pi\ \Delta x}, \qquad \alpha_y = \eta\frac{0.06}{300\pi\ \Delta y}, \qquad \alpha_z = \eta\frac{0.06}{300\pi\ \Delta z} \tag{1.30}$$

where $\eta = 1$. We should point out that if we change the width of the excitation pulse while keeping the cell size unchanged, there will be significant reflection

from the PML layer, and therefore the value of α should be a function of the width of the excitation pulse. A recommended choice for α, expressed in terms of η, is

$$\eta = \begin{cases} \dfrac{1}{1 + 0.6(\lambda_{\min} - \lambda_{\text{ref}})/\lambda_{\text{ref}}}, & \lambda_{\min} > \lambda_{\text{ref}} \\ 1 & \lambda_{\min} = \lambda_{\text{ref}} \\ \dfrac{1}{1 + (\lambda_{\text{ref}} - \lambda_{\min})/\lambda_{\text{ref}}}, & \lambda_{\min} < \lambda_{\text{ref}} \end{cases} \tag{1.31}$$

where λ_{ref} is the shortest wavelength in the spectrum of the reference excitation pulse and $\lambda_{\min}$ is the shortest wavelength in the FDTD simulations. It is useful to point out that we have introduced α in the time-convolution PML to improve performance at the lower frequencies. The reflection level of this PML will revert to the same level as that of others if we set $\alpha = 0$.

The most important features of the time-convolution PML are that its update procedure is not related to the properties of the material that fills in the computational domain, and that its performance is good even at low frequencies.

REFERENCES

[1] K. Yee, "Numerical Solution of Initial Boundary Value Problems Involving Maxwell's Equations in Isotropic Media," *IEEE Transactions on Antennas and Propagation*, Vol. 14, No. 5, May 1966, pp. 302–307.

[2] A. Taflove and S. Hagness, *Computational Electromagnetics: The Finite-Difference Time-Domain Method*, 3rd ed., Artech House, Norwood, MA, 2005.

[3] W. Yu and R. Mittra, *Conformal Finite-Difference Time-Domain Maxwell's Equations Solver: Software and User's Guide*, Artech House, Norwood, MA, 2004.

[4] W. Yu, R. Mittra, T. Su, Y. Liu, and X. Yang, *Parallel Finite Difference Time Domain Method*, Artech House, Norwood, MA, 2006.

[5] W. Yu, X. Yang, Y. Liu, L.-C. Ma, T. Su, N. Huang, and R. Mittra, "New Direction in Computational Electromagnetics Solving Large Problems Using the Parallel FDTD on the BlueGene/L Supercomputer Yielding Teraflop-Level Performance," *IEEE Antennas and Propagation Magazine*, Vol. 50, No. 23, April 2008, pp. 20–42.

[6] W. Yu, Y. Liu, T. Su, and R. Mittra, "A Robust Parallel Conformal Finite Difference Time Domain Processing Package Using MPI Library," *IEEE Antennas and Propagation Magazine*, Vol. 47, No. 3, June 2005, pp. 39–59.

[7] T. Su, Y. Liu, W. Yu, and R. Mittra, "A New Conformal Mesh Generating Technique for Conformal Finite-Difference Time-Domain (CFDTD) Method," *IEEE Antennas and Propagation Magazine*, Vol. 46, No. 1, January 2004, pp. 37–49.

[8] W. Yu and R. Mittra, "A Development Technique of Finite-Difference Time-Domain (FDTD) Software Package," *IEEE Antennas and Propagation Magazine*, No. 1, February 2003, pp. 58–74.

[9] W. Yu and R. Mittra, "A Conformal FDTD Software Package for Modeling of Antennas and Microstrip Circuit Components," *IEEE Antennas and Propagation Magazine*, Vol. 42, No. 5, October 2000, pp. 28–39.

[10] W. Yu and R. Mittra, "A Conformal Finite Difference Time Domain Technique for Modeling Curved Dielectric Surfaces," *IEEE Microwave and Guided Wave Letters*, Vol. 11, No. 1, January 2001, pp. 25–27.

[11] B. Wang et al., "A Hybrid 2-D ADI-FDTD Subgridding Scheme for Modeling On-Chip Interconnects," *IEEE Transactions on Advanced Packaging*, Vol. 24, No. 11, November 2001, pp. 528–533.

[12] W. Yu and R. Mittra, "A New Subgridding Method for Finite Difference Time Domain (FDTD) Algorithm," *Microwave and Optical Technology Letters*, Vol. 21, No. 5, June 1999, pp. 330–333.

[13] M. Marrone, R. Mittra, and W. Yu, "A Novel Approach to Deriving a Stable Hybrid FDTD Algorithm Using the Cell Method," *Proc. IEEE AP-S URSI*, Columbus, OH, 2003.

[14] T. Namiki, "A New FDTD Algorithm Based on Alternating-Direction Implicit Method," *IEEE Transactions on Microwave Theory and Techniques*, Vol. 47, No. 10, October 1999, pp. 2003–2007.

[15] F. Zheng, Z. Chen, and J. Zhang, "Toward the Development of a Three-Dimensional Unconditionally Stable Finite-Difference Time-Domain Method," *IEEE Transactions on Microwave Theory and Techniques*, Vol. 48, No. 9, September 2000, pp. 1550–1558.

[16] Y. Chao, Q. Cao, and R. Mittra, *Multiresolution Time Domain Scheme for Electromagnetic Engineering*, Wiley, New York, 2005.

[17] Q. Liu, "The PSTD Algorithm: A Time-Domain Method Requiring Only Two Cells per Wavelength," *Microwave and Optical Technology Letters*, Vol. 15, 1997, pp. 158–165.

[18] C. Guiffaut and K. Mahdjoubi, "A Parallel FDTD Algorithm Using the MPI Library," *IEEE Antennas and Propagation Magazine*, Vol. 43, No. 2, April 2001, pp. 94–103.

[19] R. Courant, K. Friedrichs, and H. Lewy, "Uber die partiellen Differenzengleichungen der mathematischen Physik," *Mathematische Annalen*, Vol. 100, 1928, pp. 32–74.

[20] G. Mur, "Absorbing Boundary Conditions for the Finite-Difference Approximation of the Time-Domain Electromagnetic Field Equations," *IEEE Transactions on Electromagnetic Compatibility*, Vol. 23, No. 3, 1981, pp. 377–382.

[21] K. Mei and J. Fang, "Superabsorption: A Method to Improve Absorbing Boundary Conditions," *IEEE Transactions on Antennas and Propagation*, Vol. 40, No. 9, September 1992, pp. 1001–1010.

[22] Z. Liao, H. Wong, Y. Baipo, et al. "A Transmitting Boundary for Transient Wave Analyzes," *Scientia Sinica* (Series A), Vol. 27, No. 10, October 1984, pp. 1062–1076.

[23] J. Berenger, "A Perfectly Matched Layer Medium for the Absorption of Electromagnetic Waves," *Journal of Computation*, Vol. 114, October 1994, pp. 185–200.

[24] S. Gedney, "An Anisotropic Perfectly Matched Layer-Absorbing Medium for the Truncation of FDTD Lattices," *IEEE Transactions on Antennas and Propagation*, Vol. 44, No. 12, December 1996, pp. 1630–1639.

[25] W. Chew and W. Wood, "A 3-D Perfectly Matched Medium from Modified Maxwell's Equations with Stretched Coordinates," *Microwave and Optical Technology Letters*, Vol. 7, 1994, pp. 599–604.

[26] W. Chew, J. Jin, and E. Michielssen, "Complex Coordinate Stretching as a Generalized Absorbing Boundary Condition," *Microwave and Optical Technology Letters*, Vol. 15, No. 6, August 1997, pp. 363–369.

[27] J. Roden and S. Gedney, "Convolution PML (CPML): An Efficient FDTD Implementation of the CFS-PML for Arbitrary Medium," *Microwave and Optical Technology Letters*, Vol. 27, No. 5, 2000, pp. 334–339.

EXERCISES

1.1 Formula (1.20) plays an important role in the time-convolution PML. Derive (1.20) from (1.16) to (1.19).

1.2 Develop a PML code and select the parameter $\sigma_{\max}$ in (1.28) to achieve minimum reflection from the PML layers.

1.3 To improve the reflection from the PML layers at low frequencies, you need to select a proper α value in (1.30). Develop a PML code and select a proper α value to improve PML performance at low frequencies.